Electrochromic Properties of Novel Selenophene and Tellurophene Derivatives Based on Carbazole and Triphenylamine Core.

Piotr Pander[†,‡], Radoslaw Motyka[‡], Pawel Zassowski[‡], Mieczyslaw Lapkowsk[‡, §], Agnieszka Swist[∥], Przemyslaw Data*[†,‡,§].

[†] Department of Physics, University of Durham, South Road, Durham DH1 3LE, United Kingdom

[‡] Faculty of Chemistry, Silesian University of Technology, M. Strzody 9, 44-100 Gliwice, Poland

[§] Center of Polymer and Carbon Materials, Polish Academy of Sciences, M. Sklodowskiej-Curie 34, 41-819 Zabrze, Poland

[∥] Wroclaw University of Technology, Faculty of Chemistry, Wybrzeze Wyspianskiego 27, 50-370 Wroclaw, Poland

ABSTRACT

2,7- and 3,6- substituted carbazole and triphenylamine chalcogenophene (Se, Te) derivatives and their electrodeposited polymers are investigated using electrochemical and UV-Vis-NIR / ESR spectroelectrochemical methods. Major differences in the case of oxidation and electropolymerization behavior between monomers and related polymers are shown. Se and Te atoms do not conjugate their lone electron pairs with the π-conjugated system and therefore only increase the contribution of the quinoid form of chalcogenophene unit. 2,7-substituted carbazole derivatives present stronger carbazole-chalcogenophene conjugation than 3,6-substituted derivatives. One 3,6- substituted carbazole derivative and triphenylamine derived polymers were found to have promising electrochromic properties with black electrochromism.

1. Introduction

Chalcogens (oxygen, sulfur, selenium, tellurium) form five-membered heterocyclic compounds named: furane, thiophene, selenophene, tellurophene respectively,[1] and are commonly used as heterocycle building blocks in order to modify electrochromism, band-gap or conductivity of small molecules and conjugated polymers.[2-4] Heteroatoms like sulfur, oxygen, nitrogen etc. change electronic properties of the conductive polymer when their lone electron pair is conjugated with the rest of the molecule in particular with the molecular backbone. However, aromatic character of these five-membered heterocyclics decreases in order O > S > Se

> Te,[3,5-8] therefore, the influence of a chalocogen's lone electron pair decreases with its increasing atomic radius. Subsequently, larger atoms in the chalcogen series such as selenium and tellurium force quinoid structures to be more likely in chalcogenophene heterocyclics. Furthermore, the electronegativity of selenium and tellurium atoms is lower than of S (2.4, 2.1, 2.5 respectively) – so tellurium behaves more like a σ-donor towards carbon.[9,10] It was shown that thiophene, selenophene, and tellurophene or their alkylated derivatives and also other derivatives may form polymers themselves or can be an important unit in a bigger structure.[2,3,11-22] While charge transfer in conductive polymers is mainly due to a hoping mechanism,[23] labile lone electron pairs of large selenium and tellurium atoms should increase material conductivity. Incorporation of selenium and tellurium instead of sulfur has therefore created materials with promising properties for application in OPVs and OFETs,[24-26] however electrochromic properties have also been studied.[27]

Carbazole, triphenylamine and thiophene are typical building blocks for conductive polymers.[28-32] As thiophene-based polymers are mainly used in organic electronic applications, while selenophene- and especially tellurophene-based polymers are still relatively uncommon.

In this paper, several carbazole and triphenylamine derivatives containing selenophene and tellurophene units are characterized, with results then compared with the data reported in the literature for similar thiophene analogs. [33-36] Both the effect of the type of chalcogen atom and also the substitution position on the carbazole (2,7- and 3,6-) are considered in this analysis. Electrochemistry (cyclic voltammetry - CV) and UV-Vis-NIR / EPR spectroelectrochemistry are used to characterize both presented monomers and electrodeposited polymer films made from the same monomers (Figure 1).
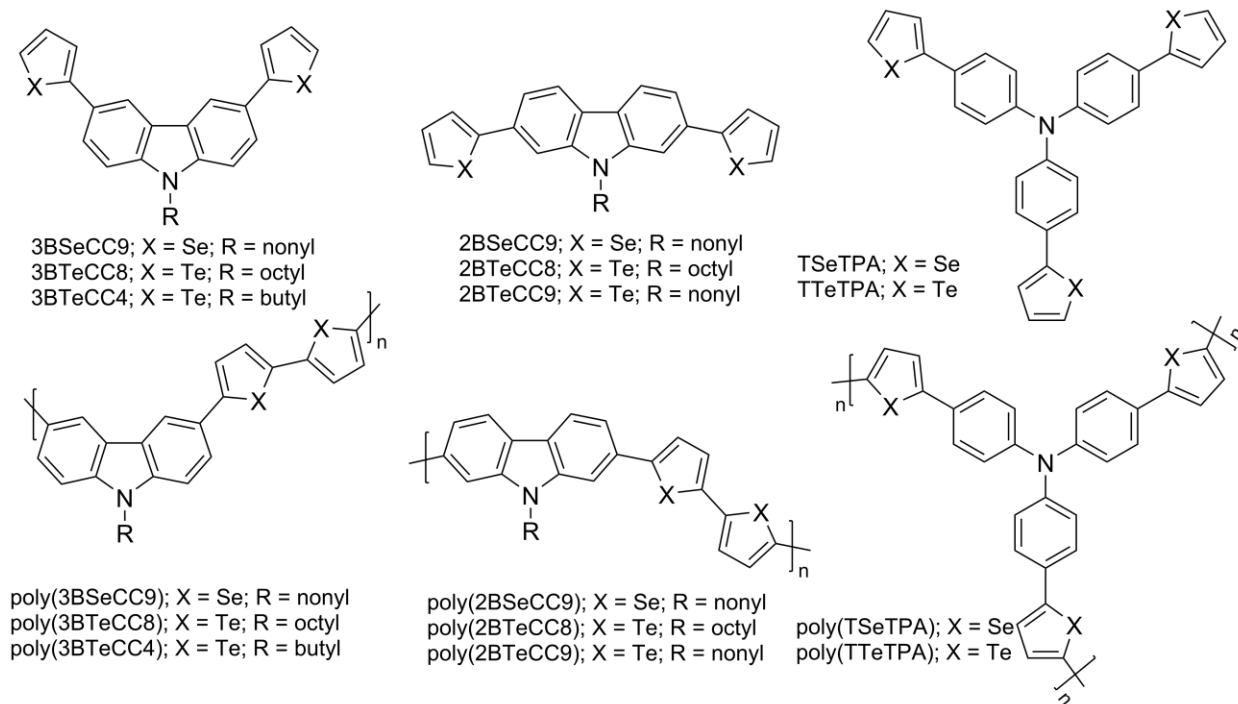
Figure 1. Structures of investigated compounds (top) and proposed structures of electrodeposited polymers (bottom). Representative molecules are discussed in the main text, results for other molecules are shown in SI.

2. Results and Discussions

As it was mentioned in the introduction, tellurophene derivatives display lower oxidation potentials and smaller band-gaps than those compounds that contain selenium. UV-Vis spectra and emission of investigated compounds are consistent with this statement. Se and Te analogs have similar measured absorption spectra, however, all tellurium-containing compounds are red-shifted compared to selenium-containing molecules (see Figure 2). This red-shift reduces the band-gap of monomers (compared to Se-derivatives): 0.12 eV for 2,7-substituted carbazole, 0.10 eV for 3,6-substituted carbazole, and 0.13 eV for triphenylamine derivatives respectively (Table 1). Furthermore, triphenylamine derivatives have the lowest band-gaps and 3,6-linked carbazoles

the highest, while 2,7-linked derivatives have an intermediate band-gap. From this point of view, it is expected that 3,6 linked carbazoles contain reduced conjugation compared to the 2,7 linked carbazole compounds. It is not surprising that molecules presented in this study show low photoluminescence quantum yields (see Table S1) as they all bear heavy elements in their structure. Incorporation of heavy elements, such as platinium[37-39] or iridium[37,39] in some cases leads to very efficient phosphors, although some heavy atoms, such as bromine[40] or selenium[41] reduce the quantum yield of fluorescence, not necessarily facilitating emission of phosphorescence in solution. That in fact is the case in this study as selenium and tellurium induce fast intersystem crossing. Photoluminescence quantum yield (Φ_{PL}) is always larger in selenophene than in tellurophene analogs, i.e. **3BSeCC9** still shows noticeable emission, but in **3BTeCC8** no emission was recorded. As Φ_{PL} varies between groups of molecules, that suggests a variation in the contribution of the heavy atom orbitals in the excited state, i.e. if the contribution is larger, the faster the intersystem crossing and the lower Φ_{PL} is observed.
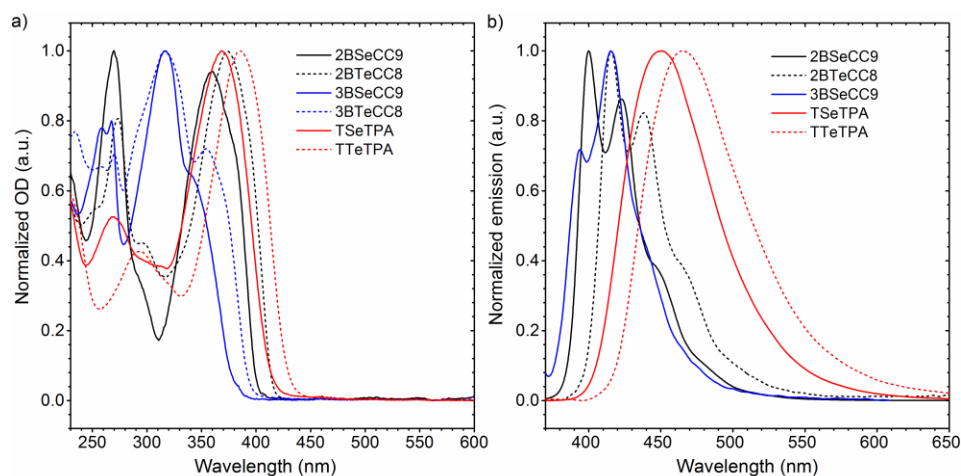

Figure 2. Normalized UV-Vis and fluorescence spectra of monomers (10^{-4} M) in dichloromethane solution. Photoluminescence quantum yields are shown in supporting information (Table S1). Please note no photoluminescence is observed for 3BTeCC8.

The electrochemical response of compounds shows that all selenophene derivatives have a higher oxidation potential than tellurophene analogs: 0.12 V for 2,7-linked carbazole, 0.08 V for 3,6-linked carbazole, and 0.03 V for triphenylamine (Table 1). It is clear that the oxidation potential of carbazole derivatives is highly affected by the presence of chalcogenophene rings, and in the case of triphenylamine derivatives the TPA unit plays the main role. In the case of carbazole derivatives, it is clear that the electrochemical anodic reaction is irreversible (see Figure 3a and b). The oxidation signals that are observed in **TSeTPA** and **TTeTPA** are mainly due to triphenylamine core and small (0.03 V) shift in oxidation potential of **TTeTPA** relative to **TSeTPA** is the consequence of the weak electron-donating behavior of tellurophene units (see Figure 3c). The anodic reaction of **TSeTPA** is partially reversible while for **TTeTPA** it is almost completely irreversible. It is known that triphenylamine itself and triphenylamine derivatives can form a stable radical cation in the process of electrochemical oxidation[30,33] and irreversibility of this process is observed in the case of **TSeTPA** and **TTeTPA**, suggesting simultaneous oxidation of chalcogenophene rings. This phenomenon is stronger pronounced for tellurophene than for selenophene due to the lower oxidation potential of the former moiety. For all presented compounds the irreversibility of anodic reaction is caused by oxidative coupling reactions resulting in deposition of insoluble oligomeric (called polymer for clarity) products upon the electrode.
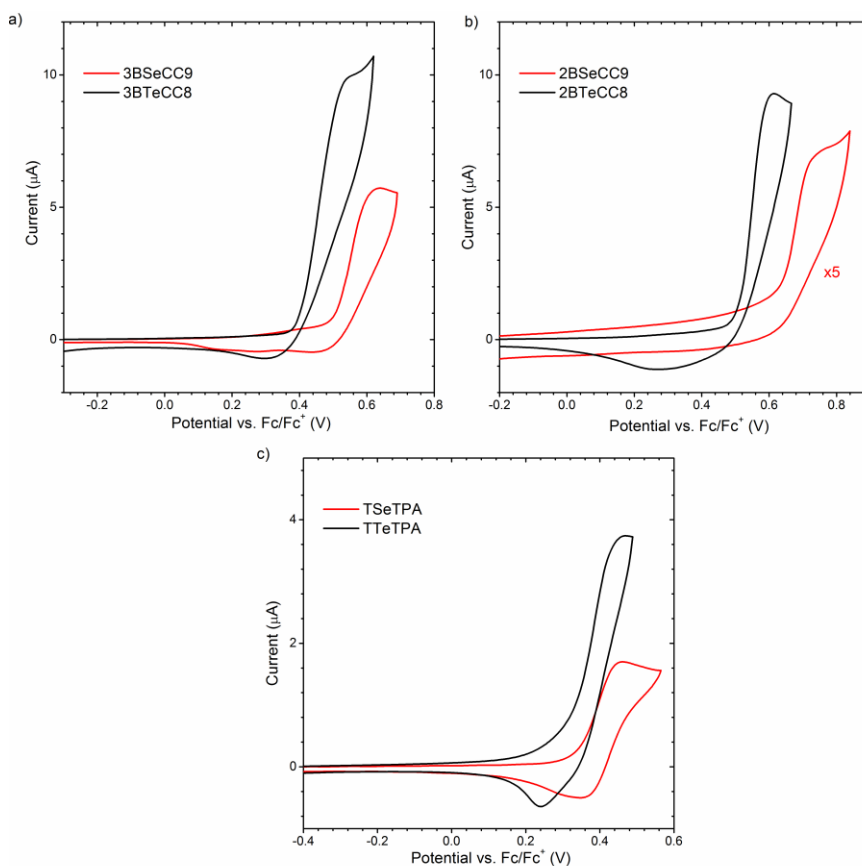
Figure 3. Cyclic voltammetry scans of investigated molecules (10^{-3} M) measured in 0.1 M Bu_4NBF_4 / dichloromethane solution. Potentials recorded relative to ferrocene/ferricinium (Fc/Fc$^+$) redox couple.

Polymer layers formed during oxidation of the presented compounds show electrochemical activity typical for conductive polymers. [33-36] While 2,7- and 3,6-linked carbazoles are expected to form linear polymers by coupling between chalcogenophene rings through the formation of bichalcogenophene bridges, triphenylamines are expected to form branched polymers due to the presence of three separated chalcogenophene units (see Figure 1 and 4).

Voltammograms (Figure 4) show that both chalcogen atom type and substitution position (for carbazoles) has an influence on electropolymerization behavior. Firstly, there is a noted

difference in polymerization between 2,7- and 3,6-linked carbazoles. 2,7-linked carbazoles polymerize at a slower pace than 3,6-linked derivatives, forming less stable polymers. This is consistent with previous literature.[32] Interestingly 2,7- and 3,6- thiophene analogs of investigated monomers both show comparable electrochemical properties. Normally electropolymerization of carbazoles occur at the 3 and 6 positions[32] and when those positions are not substituted, such as in 2,7-substituted carbazoles, some additional defects can occur in the structure of the polymer. Electropolymerization behavior of both **TSeTPA** and **TTeTPA** is very similar, however, the polymerization potential of **TSeTPA** is higher than that of **TTeTPA**.
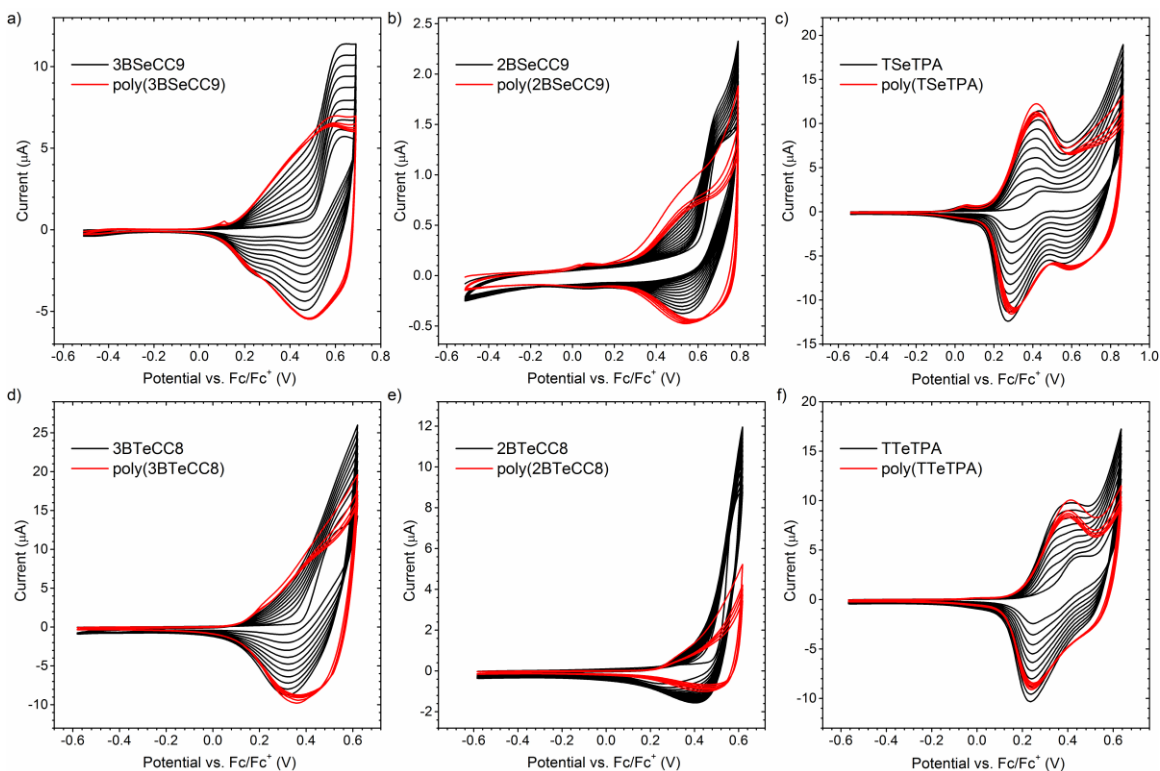

Figure 4. Electrochemical oxidative polymerization of investigated compounds *via* cyclic voltammetry (10 cycles, black lines) and electrochemical response of obtained films in electrolyte solution without monomer (5 cycles, red lines). Electrolyte solution: 0.1 M Bu_4NBF_4 in dichloromethane. Monomer concentration: 10^{-3} M. Scan rate 50 mV·s^{-1}. Potentials recorded relative to ferrocene/ferricinium (Fc/Fc$^+$) redox couple.

8

In general, all polymers have a lower oxidation onset than the corresponding monomers as a consequence of their longer conjugation length (see Table 1). Differences in oxidation onsets in the case of 3,6-linked carbazoles and for triphenylamine polymers (Se- compared to Te-containing) are negligible and therefore may be assumed to be almost equal. Tellurium derivatives generally have lower optical band-gaps than selenium analogs. However, carbazole derivatives contain almost identical electron affinity regardless the type of the chalcogen. Heavier chalcogen atoms push the ionization potential down in those compounds without any change in electron affinity. In triphenylamine derivatives, the first electron is donated by the TPA unit, therefore the ionization potential remains almost constant while the Te atom in the molecular structure increases the electron affinity of the molecule in relation to the Se-containing derivative. In the case of the polymers, the results are not as clear as for monomers, however, a similar trend is observed. In particular, triphenylamine polymers behave similar to related monomers, therefore poly(**TSeTPA**) has a lower electron affinity than poly(**TTeTPA**) and a wider band-gap whereas both polymers have almost identical ionization potential.

Table 1. Electrochemical and spectroscopic characteristics of investigated compounds. E_g^{op} – optical band-gap; E_{ox}^{CV} – *onset* oxidation potential measured with CV; IP – ionization potential; EA – electron affinity, $IP = E_{ox}^{CV} + 5.1$; An equation $EA = IP - E_g^{op}$ is used to estimate electron affinity. Potentials used in calculations were recorded relative to ferrocene/ferricinium (Fc/Fc$^+$) redox couple.

Compound / polymer	E_g^{op} (eV)	E_{ox}^{CV} (V)	IP (eV)	EA (eV)
2BSeCC9	3.11	0.63	5.73	2.62
3BSeCC9	3.25	0.48	5.58	2.34
TSeTPA	3.02	0.34	5.44	2.42
2BTeCC8	2.99	0.51	5.61	2.62
3BTeCC8	3.15	0.40	5.50	2.35
TTeTPA	2.89	0.31	5.41	2.52
poly(**2BSeCC9**)	2.24	0.29	5.39	3.14
poly(**3BSeCC9**)	2.41	0.14	5.24	2.83
poly(**TSeTPA**)	2.25	0.22	5.32	3.07
poly(**2BTeCC8**)	2.10	0.24	5.34	3.24
poly(**3BTeCC8**)	2.39	0.14	5.24	2.85
poly(**TTeTPA**)	2.05	0.21	5.31	3.26

Electrodeposited polymer layers present interesting electrochromic properties (Figure 5). Firstly, both 2,7-substituted carbazoles give almost non-electrochromic polymers (Figure 5c and d), whereas 3,6-linked forms of the polymers display electrochromism (Figure 5a and b). A more in-depth analysis of poly(**2BSeCC9**) and poly(**2BTeCC8**) can subsequently be found in Figure S1 and S2). Surprisingly both 2,7- and 3,6-bithiophene carbazole-based polymers show

significant electrochromism. [35,42] As proposed in Scheme S3 both 3,6-linked carbazole and triphenylamine polymers form, upon oxidation, radical cations with similar conjugation pattern, thus similar electron density distribution. Such a conjugation pattern, being similar to polyaniline, with chalcogenophene in *para* position to nitrogen, can be considered as polyaniline-like. This kind of pattern is a strong chromophore. On the other hand, 2,7-linked carbazoles adapt a different conjugation pattern with the second phenyl ring of carbazole being situated in *para* position to chalcogenophene. In this case two phenyl rings of carbazole are likely to be conjugated through double C=C bond, promoting a biphenyl-like pattern. As shown above, differences in electron density between 2,7-linked and 3,6-linked carbazoles in the oxidized form directly affect their electrochromic properties. Better contrast between oxidised and reduced state present, in general, selenophene analogs (with the same linking type) – especially poly(**3BSeCC9**).

Oxidation of poly(**3BSeCC9**) (Figure 5a) leads to the formation of polarons (from 0.1 V to 0.6 V vs. Fc/Fc$^+$), followed by the creation of bipolarons at higher voltages (from 0.6 V to 1.1 V vs. Fc/Fc$^+$). This polymer, therefore, shows typical doping-dedoping behavior. Polaronic states are indicated by broad absorption bands (λ = 500-800 nm and λ > 850 nm). The bipolaronic band ($\lambda_{max} \approx$ 980 nm) is formed in the second stage (over 0.6 V). It is noted that oxidation of the polymer film leads to a decrease of neutral polymer absorption bands (λ < 490 nm) and the observed process is reversible with an isosbestic point at $\lambda \approx$ 470 nm. Poly(**3BTeCC8**) (Figure 5b) has similar electrochromic properties to poly(**3BSeCC9**), however, the formation of bipolaronic states is not observed, instead polymer degradation occurs at higher applied potentials. The polaronic absorption band that is observed is broad and similar to that of the

selenophene analog. The electrochromic response is reversible with an isosbestic point at $\lambda \approx 430$ nm.
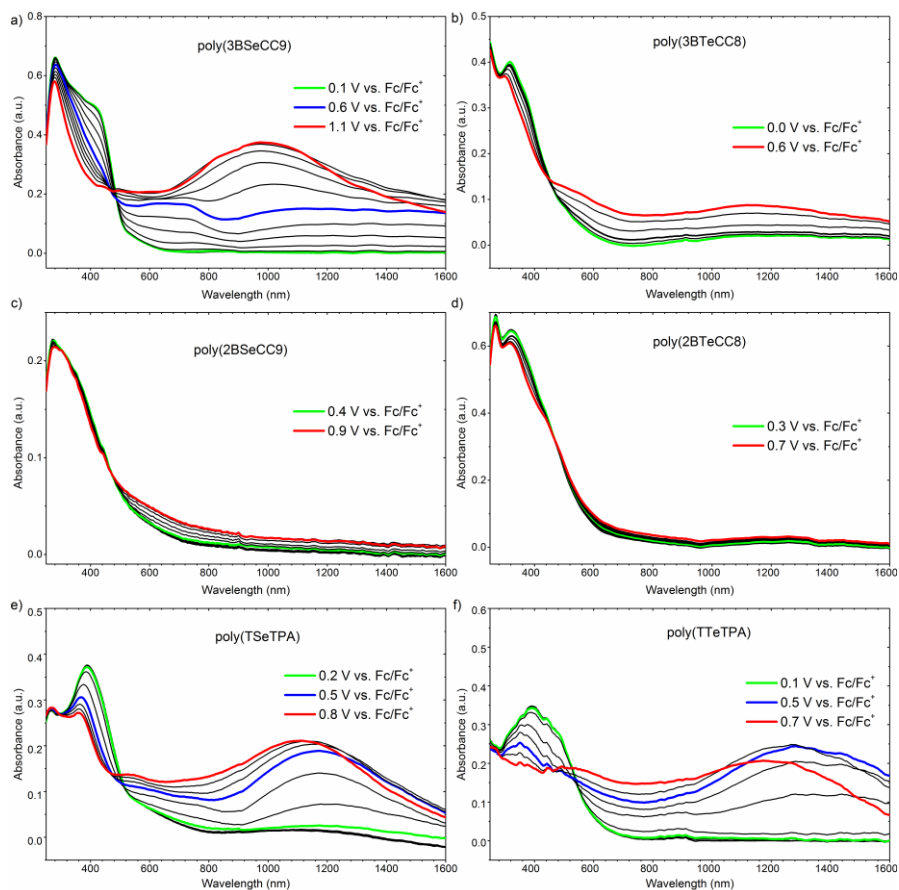

Figure 5. UV-Vis-NIR spectroelectrochemical characterization of polymer layers obtained on an ITO coated quartz electrode. Selected spectra are highlighted (color), where green denotes the spectrum of a neutral polymer, the red spectrum at maximum applied potential, and blue an intermediate stage if present. Measurements were conducted in 0.1 M dichloromethane solution of Bu_4NBF_4. Potentials recorded relative to ferrocene/ferricinium (Fc/Fc^+) redox couple.

Triphenylamine polymers, poly(**TSeTPA**) and poly(**TTeTPA**) (Figure 5e and f), both have similar electrochromic properties, however, there are some differences due to different chalcogenophene atoms contained. The main differences are shapes and maxima of the

absorption bands. In particular, the polaronic band of poly(**TTeTPA**) ($\lambda_{max} \approx 1280$ nm) is red-shifted compared to poly(**TSeTPA**) ($\lambda_{max} \approx 1170$ nm). It is observed that both polymers do not show exact isosbestic points, and pseudo-isosbestic points are placed in 500-530 nm region. Regardless of this feature, both polymers present good reversibility of the doping-dedoping process. Poly(**TTeTPA**) seems to be a more promising polymer than poly(**TSeTPA**), due to its more pronounced electrochromic response in the UV-Vis region and almost flat absorption spectrum in the region of 400-800 nm, indicating a gray/black colored film.

As a part of stability analysis, the EPR spectroelectrochemistry was conducted. All investigated compounds give species with an unpaired electron as a result of oxidation (Figure 6). Observed structureless EPR spectra are the consequence of both strong delocalization of unpaired electron and low stability of the radical, however, the presence of heavy selenium and tellurium atoms could also explain this phenomenon. Structureless spectra provide no information about the cation-radical structure, therefore only the gyromagnetic factor (*g*-factor) and signal width can be analyzed. Radical cations of aryl amines usually are characterized by a g-factor higher than 2.0030, due to the presence of spin density on nitrogen atom.[30,43-45] However, it is worth noting that some authors reported lower values.[46] Spectra from oxidized triphenylamine derivatives (Table 2) show the lowest *g*-factor values, in the range of 2.0020-2.0025 that are more typical for aromatic radicals without heteroatoms.[49] Taking above into account a strong delocalization of radical species on the carbon backbone occurs with small contribution of the nitrogen atom. In the case of carbazole derivatives, the *g*-factor observed suggests a noticeable nitrogen atom contribution – phenylaminyl radical has a *g*-factor in the range of 2.0031-2.0035. It can, therefore, be concluded for such derivatives the radical is delocalized on both chalcogenophene units and the carbazole unit.
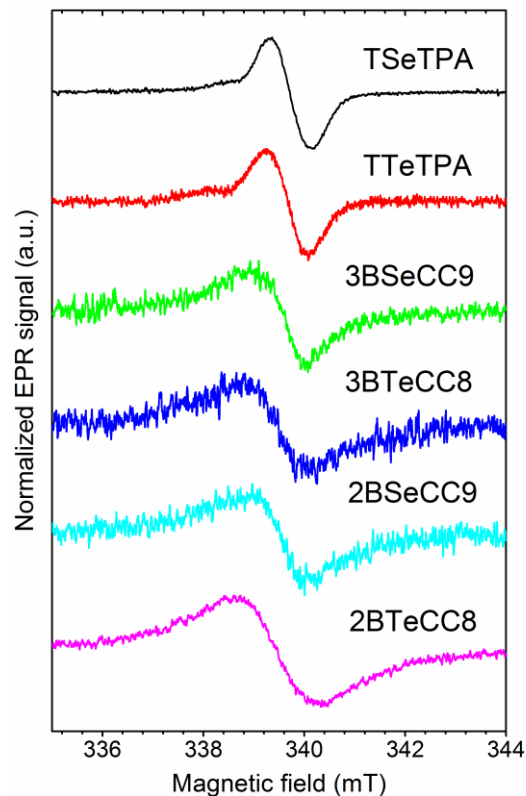
Figure 6. Normalized EPR spectra of radical cations formed during oxidation of investigated compounds to the first oxidation peak. Spectra measured in 0.1 M Bu$_4$NBF$_4$ / DCM solution. Compound concentration: 10^{-3} M.

It was previously shown that chalcogen atoms in chalcogenophenes have no direct contribution to the cation-radical structure (ie. contribution to *g*-factor), however they do change the contribution of quinoid form of the chalcogenophene ring (which is small for furan and high for tellurophene).[50] Therefore it is expected that there is no influence of chalcogenophene atom on g-factors of analyzed radicals. However, it was found that selenium and tellurium atoms broaden the EPR signal and the signals of the tellurophene derivatives are wider than those of containing selenium. Additionally, this broadening effect depends on the strength of the electron – chalcogenophene interaction, and therefore triphenylamines are expected to have the lowest

14

contribution from the chalcogenophene rings to the spin density, as the radical is mostly associated with the triphenylamine. Among the carbazoles, the slightly wider signals of the 2,7 – substituted derivatives may suggest increased conjugation between chalcogenophene units and the carbazole than 3,6 – substituted compounds.

Table 2. Gyromagnetic factors and signal width of cation radicals of monomers.

Compound	g-factor	Peak-to-peak signal width (mT)
TSeTPA	2.0023	0.95
TTeTPA	2.0022	0.97
3BSeCC9	2.0030	1.17
3BTeCC8	2.0032	1.51
2BSeCC9	2.0033	1.24
2BTeCC8	2.0032	1.65

EPR spectroelectrochemistry is a very useful tool to study charge carrier formation in conductive polymer films. However, selenium and tellurium atoms have a strong influence on EPR signal width, therefore signals are broad and relatively weak. This phenomenon is a consequence of the high mass of the chalcogen nucleus and large number of electrons surrounding the atom, as the unpaired electron can interact with them. Interestingly, thiophene analogs of investigated polymers show much narrower EPR signals.[35] All investigated polymers that give a signal in EPR spectroscopy after doping, leave some remnants of the doped species after dedoping. It was found that those species cannot be completely removed from the polymer – the polymer remains virtually doped. These remaining polarons or radicals may be in this case

interpreted as defects in the polymer structure, such as radicals formed by overoxidation of some chalcogenophene rings. As UV-Vis-NIR spectroelectrochemistry shows, the radical remnants do not contribute to the electrochromic response of polymers. Similar behavior has been observed in the case of some polymers with 3,4-ethylenedioxythiophene or thiophene units,[35,51] but also in selenophene-containing structures.[41] Initial value for the *g*-factor (g = 2.0040) for poly(**3BSeCC9**) (Figure S4) shows that the residual spins are placed on the carbazole units. Oxidation of the film results in the formation of polarons, which is indicated by an increase in spin concentration at 0.1 V potential (Figure 7c) and in the narrowing of the signal over 0.05 V (Figure 7a and S3). Polarons that are formed in the first stage of oxidation are delocalized on the carbon atoms of bichalcogenophene units, which is concluded from a *g*-factor drop (*g* = 2.0024 at 0.3 V). In the second step of oxidation, the carbazole units are oxidized which can be concluded from gradual increase of the *g*-factor over 0.3 V potential. Formation of bipolarons can also be noted in this step because the relative spin concentration starts to lower its gradient of increase with potential and furthermore, a broadening of the EPR signal is observed. Formation of bipolarons agrees with the results obtained *via* UV-Vis-NIR spectroelectrochemistry. Doping and dedoping half cycles are almost identical which indicates moderate stability of the polymer film and reversibility of the process.

The initial *g*-factor of the radicals in poly(**3BTeCC8**) derivative (*g* = 2.0025, Figure S7) suggests a small interaction of the radical with the nitrogen atom, therefore the remaining species may be located on bitellurophene units. An increase of the relative spin concentration starts at 0.1 V potential (Figure S5), but the increase of the g-factor and signal width starts at 0.3 V potential (Figure S6 and S7). This shows that bitellurophene units are oxidized in the first stage while in the second stage, the oxidation of carbazole units takes place. The spin concentration

stabilizes at 0.5-0.6 V potential which is due to the formation of bipolarons. **2BSeCC9** polymerizes slowly and the obtained film is thin, resulting in a weak signal, affected by noise (Figure S8). The initial g-factor (about 2.0040) has a similar value to poly(**3BSeCC9**) (Figure S10), but after electrochemical doping of the polymer, this value decreases only to 2.0036 which indicates an interaction of the spin with a nitrogen atom. This phenomenon can be explained by good conjugation between carbazole and biselenophene units in the 2,7 position. At a potential of 0.3-0.4 V, both signal width and g-factor start to increase (Figure S9 and S10) which can be attributed to the formation of polarons on carbazole units which may cause polymer degradation (note free 3 and 6 positions of the carbazole unit). A similar phenomenon in the case of the tellurophene derivative has not been observed, here the g-factor remains virtually constant at any potential applied. The location of the radical on the carbazole units may lead to side reactions causing degradation due to the unsubstituted 3 and 6 positions on the carbazole unit. The specific behavior of poly(**2BTeCC8**) is noteworthy. The film has a strong EPR signal (Figure 7b and d) and the g-factor of the radical does not change significantly during doping, and only fluctuates in the range of $g = 2.0033 - 2.0036$ (Figure S12). This fact shows that the radical formed does not change the structure during doping / dedoping half cycles. This is probably the reason for the better stability of the film than in the case of poly(**2BSeCC9**). A slight but noticeable broadening of the signal with the increase of the applied potential (Figure S11) can be attributed to the formation of a small number of bipolarons. At the beginning of oxidation of the poly(**TSeTPA**) film, the g-factor drops rapidly ($g = 2.0017$ at 0.5 V) with an increase of spin concentration (Figure S13 and S15) which indicates the formation of radicals on triphenylamine units. The radical has low g-factor value due to the small interaction of the radical with the nitrogen atom. Further oxidation leads to an increase in g-factor, which can be attributed to oxidation of the

biselenophene units. Small potential splitting between the oxidation of triphenylamine and biselenophene units should be noted. It is expected that in the case of poly(**TTeTPA**), the potential splitting is negligible, which can explain its behavior (see text below). Doping and dedoping half cycles show perfect reversibility of the process (Figure S13). After several attempts of successful doping and dedoping it was found that poly(**TTeTPA**) does not show an EPR signal or the signal is extremely weak. This behavior can suggest simultaneous oxidation of triphenylamine and bitellurophene units, which results in the instant formation of bipolarons while the polymer is being doped.
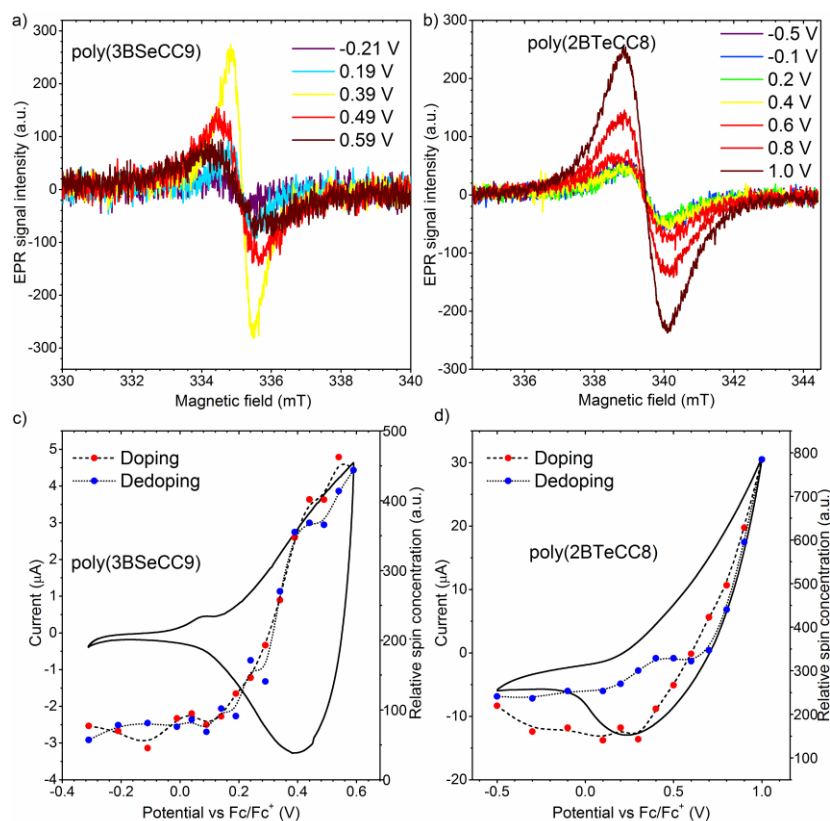

Figure 7. Selected EPR spectra measured during doping a thin film of a) poly(**3BSeCC9**) and b) poly(**2BTeCC8**). Relative spin concentration during doping (red circles) and dedoping (blue circles) of a thin film of c)

poly(**3BSeCC9**) and d) poly(**2BTeCC8**). Recorded in 0.1 M Bu$_4$NBF$_4$ / DCM supporting electrolyte solution.

Potentials recorded relative to ferrocene/ferricinium (Fc/Fc$^+$) redox couple.

As a final part of analysis, the electrochromic properties were analysed based on the electrochemically synthesized polymer. The 2,7-bichalcogenophene carbazoles analysed in this work have a mediocre electrochromic response and are not further investigated in terms of electrochromism. Poly(**3BTeCC8**) was found to be relatively the least stable polymer among all investigated with a significant electrochromic response. As a result, only poly(**TSeTPA**), poly(**TTeTPA**), and poly(**3BSeCC9**) were chosen for further investigation with high-speed potential switching measurements (see Figure 8). Two wavelengths ranges were chosen in the experiment: first from 390-400 nm representing the neutral polymer film and the second from 650-750 nm representing the doped polymer film. The potential switching measurement enables the investigation of polymer film stability in doping-dedoping cycles by comparing the optical contrast between the doped and dedoped film in the first and last cycle (here the 24th). Therefore it can be stated that the stability of the three polymers follows the order: poly(**3BSeCC9**) > poly(**TSeTPA**) > poly(**TTeTPA**) and the optical contrast equals 90%, 78-79%, and 65-71% of the initial values respectively.
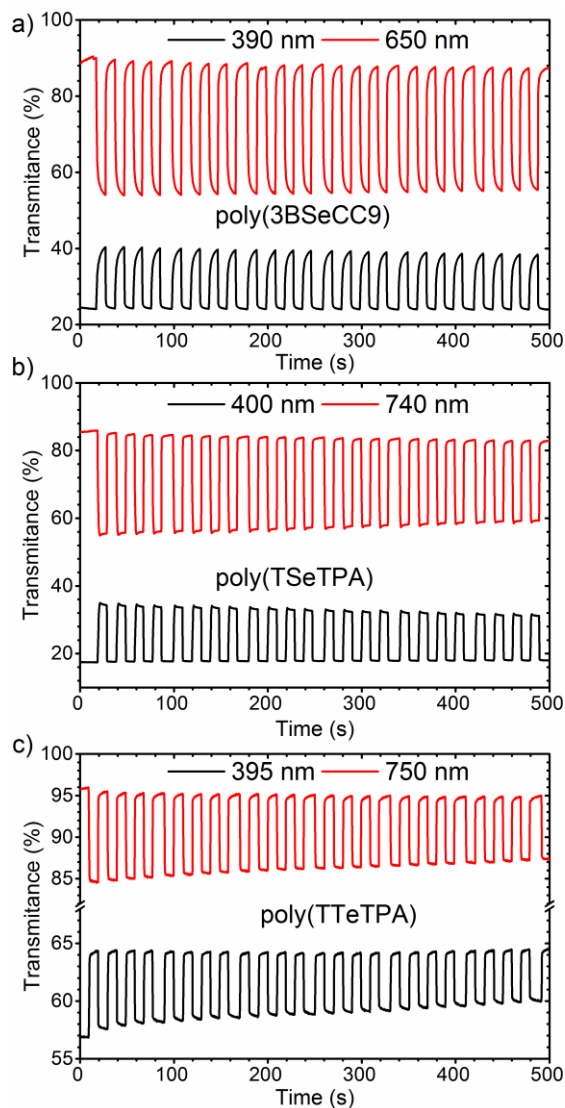
Figure 8. Electrochromic switching response of a) poly(**3BSeCC9**), b) poly(**TSeTPA**), and c) poly(**TTeTPA**) films on ITO on quartz electrode in 0.1 M Bu₄NBF₄ / dichloromethane solution. Potentials applied for doping / dedoping (vs. Fc/Fc⁺): poly(**3BSeCC9**) 0.65 V / -1.15 V; poly(**TSeTPA**) 0.5 V / -1.2 V; poly(**TTeTPA**) 0.4 V / -1.2 V. Potential step duration: 10 s. Potentials recorded relative to ferrocene/ferricinium (Fc/Fc⁺) redox couple.

The switching measurements (see Table 3) show that the doping process is generally slower than dedoping. Furthermore, polaronic bands react faster than neutral polymer bands during doping, whereas during dedoping bands swap the reaction time order. In general, the oxidized form of all

selected polymers displays a black/gray color, while various colors are found in the neutral polymer forms. With this in mind, poly(**3BSeCC9**) was found to have the most promising properties, with relatively high coloration efficiency (CE) at both investigated wavelengths (over 180 cm^2·C^{-1}) and good stability. It is expected that poly(**3BSeCC9**) has a very high CE at $\lambda_{max} \approx$ 980 nm as the CE depends on ΔOD (Optical Density) between the oxidized and neutral film, however, infrared absorption bands are not applicable for electrochromic devices.

Table 3. Electrochromic properties of investigated polymers. λ – investigated wavelength; T_{ox} – transmittance of oxidized film at λ; T_{red} – transmittance of neutral film at λ; ORT$_{dop}$ – Optical Response Time of the film during doping; ORT$_{dedop}$ – Optical Response Time of the film during dedoping; ΔOD – difference of optical density between neutral and oxidized film at λ; Q_D – charge density calculated in chronoculometric experiment; CE – coloration efficiency; CR – contrast ratio. For further information please see previous works.[13,35, 47,48]

Polymer	λ (nm)	T_{ox} (%)	T_{red} (%)	ORT$_{dop}$ (s)	ORT$_{dedop}$ (s)	ΔOD (-)	Q_D (mC·cm^{-2})	CE (cm^2·C^{-1})	CR (-)
poly(3BSeCC9)	650	89.5	54.1	4.86	2.48	0.22	1.20	181.9	1.65
	390	24.1	40.2	6.51	1.75	-0.22	1.20	184.9	0.60
poly(TSeTPA)	740	85.5	55.7	1.62	0.67	0.19	2.59	72.0	1.54
	400	17.4	34.4	1.78	0.54	-0.30	2.59	114.5	0.51
poly(TTeTPA)	750	95.5	84.6	0.98	1.22	0.05	0.84	62.7	1.13
	395	57.6	64.5	4.12	0.34	-0.05	0.84	58.5	0.89

3. Conclusions

Presented 3,6- and 2,7- substituted carbazole derivatives and triphenylamine derivatives were found to undergo oxidative electropolymerization with the formation of electroactive films. Polymer films thus obtained were investigated by spectroelectrochemical techniques. It was

shown that 2,7- substituted carbazole polymers are not electrochromic while 3,6- substituted and triphenylamine polymer derivatives show satisfactory electrochromism. One of the polymers: poly(**3BSeCC9**) was found to have very promising properties for applications in electrochromic devices.

The increase of chalcogen atomic number indicates lower band-gaps of both monomers and polymers. It was observed that a decrease of optical band-gap of carbazole derivatives is therefore due to a lowering of the ionization potential of the molecule while electron affinity does not change. In the case of triphenylamine derivatives, it is observed that chalcogen atom type affects only electron affinity, while ionization potential remains almost the same.

EPR spectroelectrochemical measurements show different structures of cation-radicals formed by both carbazole and triphenylamine polymers and their related monomers. It was shown that stronger conjugation between carbazole and chalcogenophene substituents is present when the carbazole is 2,7- substituted whereas in the 3,6- substituted compound, conjugation is relatively weak. The chalcogen atom does not participate in the structure of the radical, it only increases the quinoid form of chalcogenophene ring decreasing its aromaticity. The increase of chalcogen atomic number makes this effect stronger.

4. Experimental section

All electrochemical studies were conducted in Ar purged 0.1 M solutions of electrolyte Bu_4NBF_4, 99% (Sigma-Aldrich) in dichloromethane solvent, (Sigma-Aldrich, for HPLC) at room temperature. The electrochemical cell was comprised of a 1 mm diameter platinum disk (CV), platinum wire (electron paramagnetic resonance (EPR)), or indium tin oxide (ITO) coated quartz (for UV–Vis-NIR) as the working electrode, silver wire as the quasi-reference electrode,

and a platinum wire as the auxiliary electrode. In each electrochemical experiment, the reference electrode potential was monitored using ferrocene as an internal standard. CV investigations were carried out using an Autolab PGSTAT20 potentiostat using a scan rate of 50 mV·s^{-1} (oxidation, electropolymerization, and multiple doping–dedoping processes). All electrochemical measurements were performed at a concentration of 1.0×10^{-3} M for the investigated compounds. UV-Vis-NIR spectroelectrochemistry was carried out using QE6500 and NIRQuest detectors (Ocean Optics). In situ EPR spectroelectrochemical experiments were performed using a Jeol JES-FA200 spectrometer coupled with an Autolab PGSTAT 100N potentiostat. The g-factor value was determined by comparison with a JEOL internal standard (Mn(II) salt). Absorption and photoluminescence spectra were collected using a UV-3600 double beam spectrophotometer (Shimadzu), and a Fluorolog spectrofluorometer (Jobin Yvon).

AUTHOR INFORMATION

Corresponding Author

*E-mail: Przemyslaw.Data@dur.ac.uk

REFERENCES

(1) Salzner, U.; Langowski, J.B.; Pickup, P.G.; Poirier, R.A. Comparison of geometries and electronic structures of polyacetylene, polyborole, polycyclopentadiene, polypyrrole, polyfuran, polysilole, polyphosphole, polythiophene, polyselenophene and polytellurophene. *Synth. Met.* **1998**, *96*, 177-189.

(2) Data, P.; Lapkowski, M.; Motyka, R.; Suwinski J. Influence of heteroaryl group on electrochemical and spectroscopic properties of conjugated polymers. *Electrochim. Acta* **2012**, *83*, 271-282.

(3) Ashraf, R.S.; Meager, I.; Nikolka, M.; Kirkus, M.; Planells, M.; Schroeder, B.C.; Holliday, S.; Hurhangee, M.; Nielsen, C.B.; Sirringhaus, H.; McCulloch, I. Chalcogenophene Comonomer Comparison in Small Band Gap Diketopyrrolopyrrole-Based Conjugated Polymers for High-Performing Field-Effect Transistors and Organic Solar Cells. *J. Am. Chem. Soc.* **2015**, *137*, 1314-1321.

(4) Takimiya, K.; Konda, Y.; Ebata, H.; Niihara, N.; Otsubo, T. Facile Synthesis, Structure, and Properties of Benzo[1,2-b:4,5-b']dichalcogenophenes. *J. Org. Chem.* **2005**, *70,* 10569-10571.

(5) Lukevics, E.; Arsenyan, P.; Belyakov, S.; Pudova, Molecular Structure of Selenophenes and Tellurophenes. *Chem. Heterocycl. Compd.* **2002**, *38*(7), 763-777.

(6) Jung, E.H.; Bae, S.; Yoo, T.W.; Jo, W.H. The effect of different chalcogenophenes in isoindigo-based conjugated copolymers on photovoltaic properties. *Polym. Chem.* **2014, 5,** 6545-6550.

(7)   Kaur, M.; Yang, D.S.; Shin, J.; Lee, T.W.; Choi, K.; Cho, M.J.; Choi, D.H. A novel tellurophene-containing conjugated polymer with a dithiophenyl diketopyrrolopyrrole unit for use in organic thin film transistors. *Chem. Commun.* **2013**, *49*, 5495-549*7.*

(8)   McCormick, T.M.; Jahnke, A.A.; Lough, A.J.; Seferos, D.S. Tellurophenes with Delocalized π-Systems and Their Extended Valence Adducts. *J. Am. Chem. Soc.* **2012**, *134*, *3*542-3548.

(9)   Dean, J.A. Lange's Handbook of Chemistry, *McGraw-Hill, Inc.* **1999**.

(10)   Patnaik, P. Handbook of Inorganic Chemicals, *McGraw-Hill, Inc.* **2003**.

(11)   Lapkowski, M; Motyka, R.; Suwinski, J.; Data, P. Photoluminescent Polytellurophene Derivatives of Conjugated Polymers as a New Perspective for Molecular Electronics. *Macromol. Chem. Phys.* **2012**, *213*, 29-35.

(12)   Data, P.; Pander, P.; Lapkowski, M.; Swist, A.; Soloducho, J.; Reghu, R.R.; Grazulevicius, J.V. Unusual properties of electropolymerized 2,7- and 3,6- carbazole derivatives. *Electrochim. Acta* **2014**, *128*, 430-438.

(13)   Data, P.; Lapkowski, M.; Motyka, R.; Suwinski, J. Influence of alkyl chain on electrochemical and spectroscopic properties of polyselenophenes. *Electrochim. Acta* **2013***, 87*, 438-449**.**

(14)   Yamamoto, T.; Sanechika, K.; Yamamoto, A. Synthesis of regioregular π-conjugated poly(thienyleneethynylene) with a hindered phenolic substituent. *J. Polym. Sci. Polym. Lett. Ed.* **1980***, 18,* 9-12.

(15) Street, G.B.; Clarke, T.C. Conducting polymers: a review of recent work. *IBM J. Res. Devel.* **1981**, *25*, 51-57.

(16) Elsenbaumer, R.; Jen, K.; Oboodi, R. Processible and environmentally stable conducting polymers. *Synth. Met.* **1986**, *15*, 169-174.

(17) Hotta, S.; Rughooputh, S.D.D.V.; Heeger, A.J.; Wudl, F. Spectroscopic studies of soluble poly(3-alkylthienylenes). *Macromolecules* **1987**, *20,* 212-215.

(18) González-Tejera, M.J.; Sánchez de la Blanca, E.; Carrillo, I. Polyfuran conducting polymers: synthesis, properties, and applications. *Synt. Met.* **2008**, *58*, 165-189.

(19) Ripoll, J.D.; Serna, A.; Guerra, D.; Restrepo, A. Electronic structure calculations on helical conducting polymers. *J. Phys. Chem. A* **2010**, *114*, 10917-10921.

(20) Patra, A.; Bendikov, M. Polyselenophenes. *J. Mater. Chem.* **2010**, *20*, 422-433.

(21) Özkut, M.I.; Atak, S.; Önal, A.M.; Cihaner, A. A blue to highly transmissive soluble electrochromic polymer based on poly(3,4-propylenedioxyselenophene) with a high stability and coloration efficiency. *J. Mater. Chem.* **2011**, *21*, 5268-5272.

(22) Das, S.; Zade, S.S. Poly(cyclopenta[c]selenophene): a new polyselenophene. *Chem. Commun.* **2010**, *46*, 1168-1170.

(23) Zuppiroli, L.; Bussac, M.N.; Paschen, S.; Chauvet, O.; Forro, L. Hopping in disordered conducting polymers. *Phys. Rev. B* **1994**, *50*, 5196-5203.

(24) Guo, X.; Baumgarten, M.; Müllen, K. Designing conjugated polymers for organic electronics. *Prog. Polym. Sci.* **2013**, *38*, 1832-1908.

(25) Gao, P.; Beckmann, D.; Tsao, H.N.; Feng, X.; Enkelmann, V.; Pisulaz, W.; Müllen, K. Benzo[1,2-b:4,5-b′]bis[b]benzothiophene as solution processible organic semiconductor for field-effect transistors. *Chem. Commun.* **2008**, *13*, 1548-1550.

(26) Jung, E.H.; Bae, S.; Yoo, T.W.; Jo, W.H. The effect of different chalcogenophenes in isoindigo-based conjugated copolymers on photovoltaic properties. *Polym. Chem.* **2014**, *5*, 6545-6550.

(27) Yang, W.; Zhao, J.; Cui, C.; Kong, Y.; Li, P. Characterization and Electrochemical Synthesize from Selenophene-Substituted Poly(Triphenylamine) as Anodically Materials for Electrochromic Devices. *Int. J. Electrochem. Sci.* **2012**, *7*, 7960-7975.

(28) Heeger, A.J. Semiconducting polymers: the Third Generation. *Chem. Soc. Rev.* **2010**, *39*, 2354-2371.

(29) Guo, X.; Baumgarten, M.; Müllen, K. Designing conjugated polymers for organic electronics. *Prog. Polym. Sci.* **2013**, *38*, 1832-1908.

(30) Su, C.; Yang, F.; Ji, L.; Xu. L; Zhang, C. Polytriphenylamine derivative with high free radical density as the novel organic cathode for lithium ion batteries. *J. Mater. Chem. A* **2014**, *2*, 20083-20088.

(31) Boudreault, P.-L.T.; Beaupre S.; Leclerc, M. Polycarbazoles for plastic electronics. *Polym. Chem.* **2010**, *1*, 127-136.

(32) Karon, K.; Lapkowski, M.; Grazulevicius J. Electrochemical and UV-Vis/ESR spectroelectrochemical properties of polymers obtained from isomeric 2,7- and 3,6- linked

carbazole trimers; influence of the linking topology on polymers properties. *Electrochim. Acta* **2014**, *123*, 176-182.

(33) Idzik, K.; Sołoducho, J.; Łapkowski, M.; Golba, S. Development of structural characterization and physicochemical behaviour of triphenylamine blocks. *Electrochim. Acta* **2008**, *53*, 5665-5669.

(34) Aristizabal, J.A.; Soto J.P.; Ballesteros L.; Munoz E.; Ahumada, J.C. Synthesis, electropolymerization, and photoelectrochemical characterization of 2,7-di(thiophen-2-yl)-N-methylcarbazole. *Polym. Bull.* **2013**, *70*, 35-46.

(35) Data, P.; Zassowski, P.; Lapkowski, M.; Domagala, W.; Krompiec, S.; Flak, T.; Penkala, M.; Swist, A.; Soloducho, J.; Danikiewicz W. Electrochemical and spectroelectrochemical comparison of alternated monomers and their copolymers based on carbazole and thiophene derivatives. *Electrochim. Acta* **2014**, *122*, 118-129.

(36) Lapkowski, M.; Data, P.; Nowakowska-Oleksy, A.; Sołoducho, J.; Roszak, S. Electrochemical characterization of alternate conducting carbazole–bisthiophene units. *Mater. Chem. Phys.* **2012**, *131*, 757-763.

(37) Yersin, H. Highly Efficient OLEDs with Phosphorescent Materials. *Wiley-VCH Verlag GmbH & Co. KGaA*, Weinheim, **2008**.

(38) Kwong, R.C.; Lamansky, S.; Thompson, M.E. Organic Light-emitting Devices Based on Phosphorescent Hosts and Dyes. *Adv. Mater.* **2000**, *12*, 1134-1138.

(39) Kamtekar, K.T.; Monkman, A.P.; Bryce, M.R. Recent Advances in White Organic Light-Emitting Materials and Devices (WOLEDs). *Adv. Mater.* **2010**, *22*, 572-582.

(40) Xue, P.; Wang, P.; Chen, P.; Yao, B.; Gong, P.; Sun, J.; Zhanga, Z.; Lu, R. Bright persistent luminescence from pure organic molecules through a moderate intermolecular heavy atom effect. *Chem. Sci.* **2016**, DOI: 10.1039/C5SC03739E.

(41) Pander, P.; Data, P.; Turczyn, R.; Lapkowski, M.; Swist, A.; Soloducho, J.; Monkman, A.P. Synthesis and characterization of chalcogenophene-based monomers with pyridine acceptor unit. *Electrochim. Acta* **2016**, *210*, 773-782.

(42) Kawabata K.; Goto, H. Dynamically Controllable Emission of Polymer Nanofibers: Electrofluorescence Chromism and Polarized Emission of Polycarbazole Derivatives. *Chem. Eur. J.* **2012**, *18*, 15065-15072.

(43) Pluczyk, S.; Zassowski, P.; Rybakiewicz, R.; Wielgosz, R.; Zagorska, M.; Lapkowski, M.; Pron, A. UV-vis and EPR spectroelectrochemical investigations of triarylamine functionalized arylene bisimides. *RSC Adv.* **2014**, *5* (10), 7401-7412.

(44) Pluczyk, S.; Zassowski, P.; Quinton, C.; Audebert, P.; Alain-Rizzo, V.; Lapkowski, M. Unusual Electrochemical Properties of the Electropolymerized Thin Layer Based on a s‑Tetrazine-Triphenylamine Monomer. *J. Phys. Chem. C* **2016**, *120* (8), 4382–4391.

(45) Bencivenni, G.; Cesari, R.; Nanni, D.; Mkami, H. El; Walton, J. C. EPR and pulsed ENDOR study of intermediates from reactions of aromatic azides with group 13 metal trichlorides. *Beilstein J. Org. Chem.* **2010**, *6*, 713–725.

(46) Matis, M.; Rapta, P.; Hartmann, H.; Dunsch, L. Highly Charged Cations from N,N,N′,N′-Tetrakis(4-aminophenyl)benzidine and Its N,N,N′,N′-Tetrakis(4-methoxyphenyl)-

Substituted Homologue Studied by Thin-Layer in Situ Electron Spin Resonance/UV-Vis-NIR Spectroelectrochemistry. *J. Phys. Chem. B* **2010**, 4451–4460.

(47) Gaupp, C.L.; Welsh, D.M.; Rauh, R.D.; Reynolds, J.R. Composite Coloration Efficiency Measurements of Electrochromic Polymers Based on 3,4-Alkylenedioxythiophenes. *Chem. Mater.* **2002**, *14*, 3964-3970.

(48) Monk, P.M.S.; Mortimer, R.J.; Rosseinsky, D.R. Electrochromism and Electrochromic Devices. *Cambridge University Press*, Cambridge, **2007**.

(49) Gerson, F.; Huber, W. Electron Spin Resonance Spectroscopy of Organic Radicals. *Wiley-VCH Verlag GmbH & Co. KGaA*, Weinheim, **2003**.

(50) Jahnke, A.C.; Spulber, M.; Neuburger, M; Palivan, C.G.; Wenger, O.S. Electronic coupling mediated by furan, thiophene, selenophene and tellurophene in a homologous series of organic mixed valence compounds. *Chem. Commun.* **2014**, *50*, 10883-10886.

(51) Moskwa, T.; Domagala, W.; Czardybon, A.; Pilawa, B.; Lapkowski, M. ESR spectroelectrochemistry of functionalised long side chain derivatives of poly(3,4-ethylenedioxythiophene). *Synth. Met.* **2005**, *152*, 189-192.

Table of Contents

X = Se, Te